Received: Added at production | Revised: Added at production | Accepted: Added at production

DOI: xxx/xxxx

ARTICLE TYPE

Age-optimal vaccination strategy for respiratory infectious disease: a constraint-dependant approach

Amira Bouhali[1,2] | **Walid Ben Aribi**[1,4] | **Slimane Ben Miled**[1] | **Amira Kebir**[1,3]

[1]BIMS, Institut Pasteur de Tunis, Université de Tunis El Manar, Tunis, Tunisia

[2]ENIT,Université de Tunis El Manar, Tunis, Tunisia

[3]IPEIT, Université de Tunis, Tunis, Tunisia

[4]School of Business, Esprit School of Business, Tunis, Tunisia

Correspondence

Corresponding author Amira Kebir,
Email: amira.kebir@pasteur.utm.tn

Present address

13, Place Pasteur, B.P. 74· 1002, Belvédère, Tunis, Tunisia

Abstract

After the vaccine implementation for COVID-19, the WHO set a unified vaccination approach to be adopted by all different countries. However, given the various constraints including vaccine availability, heterogeneous age distributions, and differing control measures across countries, questions arise about the optimality of the WHO strategy. In this study, we develop an age-structured SEIR epidemic model with vaccinated and unvaccinated compartments to optimize age-targeted vaccination strategies for COVID-19, incorporating realistic constraints. The model equilibria and the basic reproduction number R_0 are checked. Moreover, mathematical formulation and analysis of optimal control problem, are conducted. The model is calibrated to COVID-19 data and simulated to solve the optimal control problem under various vaccination and distancing scenarios. Results demonstrate that the optimal strategy strongly depends on the population age distribution and contact patterns. Findings emphasize the significance of age-specific disease transmission in designing vaccination priorities, particularly when vaccine supplies are constrained. The model provides a quantitative framework to inform optimal allocation strategies in a general way that allows to adapt the model for other infectious diseases exhibiting similar features to Covid-19.

KEYWORDS

Optimal Control, epidemiology, Vaccine, COVID-19, age-structured model

1 | INTRODUCTION

All over the world, different countries have been affected by the Covid-19 pandemic. The virus has revealed to be quite tricky to handle specially with factors like overpopulation and hyper-connectivity [1]. And in less than six months after the detection of the first cases, the world witnessed the worst health crisis of the this century. The shortage of feedback made it harder to control the disease without extreme measures: lockdown, closing of the public places... And scientists had to muddle through the intricacies of the forming bubble with the hope of quick results. Thereafter, people were constrained to nearly two years of trial and error before the vaccine implementation. Moreover, they were subject to the consequences of the lack of feedback on whatever strategy chosen for the vaccination [2]. This led the World Health Organization (WHO) to set a vaccination strategy that was applied in different countries across the world. The strategy used is a three-step approach to vaccination, where old individuals, health workers and high-risk groups of all ages, in every country are vaccinated first, followed by the full adult age group in every country and lastly extended vaccination of adolescents. [3] However, in various countries several severe waves followed the vaccination campaigns [4]. This highlighted that besides experimental and biological studies, mathematical modeling and computer sciences are also quite needed while studying any pandemic, specially to face over saturation of the hospitals that threatened both individuals' health and countries economics [5]. The seriousness of the situation, called for the use of all available tools to face it. Epidemiological models and optimal control were commonly used to provide information useful for decisions on disease prevention, surveillance, control, treatment and vaccine strategies implementation. This type of models is applied to several infectious diseases ranging from Influenza to Ebola or the ongoing COVID-19 outbreak [6,7,8,9,10,11,12]. And based on the newly-striking Covid-19 pandemic, that showed the importance of quick acting, came the idea of this work. As a matter of fact, this study offers an epidemiological model that can be applied to the range of infectious diseases presenting

common features of Covid. The model mainly aims to determine population-specific optimal vaccination strategy. The numerical simulations were conducted using Covid data as a response to the current crisis. The model elaborated is age-structured as experimental data showed that age is the most associated factor with the risk of hospitalization or death. In fact, while all age groups are affected by the infection, the incidence of severe forms and mortality is highest among the oldest population group [13]. Indeed, age structuring was commonly used when addressing the ongoing Covid-19 topic whether to discuss the effect of age distribution on the progress and fatality of the disease [14,15] or to investigate the effectiveness of the various strategies adopted to contain the ongoing Covid-19 [16,17]. The choice of this approach is mainly due to the impact of age on two key factors of disease spread: the immunity of individuals and their contact webs. Verily, the immune system deteriorates with age, losing its capacity to fight infections and diseases [18]. What is more, different age groups have different contact webs. Thus, the difference in age distributions leads to very unlike contact matrices that have a direct impact on infection transmission. Age-structured models coupled with optimal control served also to provide insight into the best control strategies [19]. Thus, to recapitulate, the aim of this work is to create feedback that can be useful for a range of age-dependent infectious diseases in the first part. The second part's objective is to use the model created to produce information about the optimal vaccination strategy and check its sensitivity to external constraints like maximal vaccination threshold, age distribution, and contact.

The model formulated consists of n age groups interacting with each other. Each class has its own mathematical SEIR model where both vaccinated and unvaccinated categories are presented, as well as its own vaccination rate as the control. For each class, the optimal vaccination rate is determined under different constraints of maximal doses. The model is then studied as an optimal control problem where the vaccination rates of each age class were used as the control, with the aim of minimizing the number of infected cases that necessitate hospitalization. The problem should be set and studied in a general way allowing to determine the optimal strategies to contain infections for other age-sensitive infectious diseases.

The document is organized as follows: in section 2, the SEIR model is formulated for the general case of n age groups. Section 3 is dedicated to the study of model dynamics. Specifically, it is disease-free equilibrium (DFE) was studied along with the basic reproductive number. The formulation of the optimal control problem and its results are given in section 4. After proving the existence of optimal control, the problem was treated numerically using the optimization suite GEKKO [20]. The numerical simulations allowed to determine the optimal vaccination strategy under different constraints of maximal vaccination threshold. They also helped investigate its sensitivity to some external factors like distancing measures and age distribution. The conclusion is drawn in section 6.

2 | STRUCTURED MODEL DESCRIPTION

In this section, we present an age-structured model where n age groups interact with each other: each one with its own SEIR model for both vaccinated and unvaccinated groups where S, E, I, and R denote respectively the proportions of susceptible, exposed (asymptomatic infectious), infected (symptomatic infectious) and removed (deceased and recovered) individuals. Thus, for an age group $i \in \{1, \dots, n\}$, the susceptible compartment S_i loses population through vaccination to the vaccinated susceptible compartment S_i^v or through exposure to the virus at a rate F_i. These individuals join the exposed E_i doomed to infection generating two categories of the unvaccinated infected I_{1i}, non-severe cases, and I_{2i}, the severe ones. Similarly, a proportion of the vaccinated susceptible exits this compartment towards the vaccinated exposed one, E_i^v, through contact with vaccinated or unvaccinated exposed or infected individuals of all age groups.

A proportion $q_{1i}^v E_i^v$ of the exposed joins the vaccinated infected of type 1, I_{1i}^v, which includes vaccinated individuals not suffering from severe COVID-19 cases. While, another proportion $q_{2i}^v E_i^v$ joins the vaccinated infected of type 2, I_{2i}^v, which comprises individuals with severe COVID-19 cases. All infected compartments $I_{ki},\ k = 1, 2$ and $I_{ki}^v,\ k = 1, 2$ lose population through death or recovery (see Figure 1). Thus, for each population $i \in \{1, \dots, n\}$, the model can be written as follows:

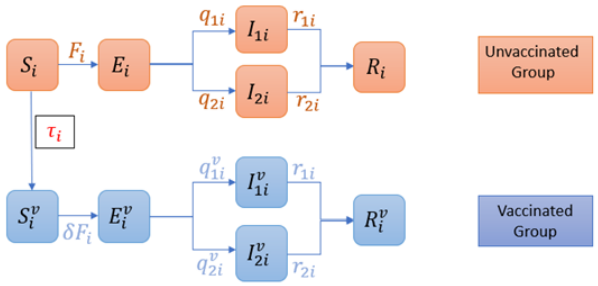

FIGURE 1 Diagram of one age class dynamics subject to model (1-10) where $F_i = \sum_{j=1}^{n}(\alpha_{1i}I_{1j} + \alpha_{2i}I_{2j} + \beta_i E_j + \alpha_{1i}^v I_{1j}^v + \alpha_{2i}^v I_{2j}^v + \beta_i^v E_j^v)d_{ij}$

$$\dot{S}_i = -F_i S_i - \tau_i S_i \tag{1}$$
$$\dot{E}_i = F_i S_i - (q_{1i} + q_{2i})E_i \tag{2}$$
$$\dot{I}_{1i} = q_{1i}E_i - r_{1i}I_{1i} \tag{3}$$
$$\dot{I}_{2i} = q_{2i}E_i - r_{2i}I_{2i} \tag{4}$$
$$\dot{R}_i = r_{1i}I_{1i} + r_{2i}I_{2i} \tag{5}$$
$$\dot{S}_i^v = \tau_i S_i - \delta F_i S_i^v \tag{6}$$
$$\dot{E}_i^v = \delta F_i S_i^v - (q_{1i}^v + q_{2i}^v)E_i^v \tag{7}$$
$$\dot{I}_{1i}^v = q_{1i}^v E_i^v - r_{1i}I_{1i}^v \tag{8}$$
$$\dot{I}_{2i}^v = q_{2i}^v E_i^v - r_{2i}I_{2i}^v \tag{9}$$
$$\dot{R}_i^v = r_{1i}I_{1i}^v + r_{2i}I_{2i}^v \tag{10}$$

where for all $i \in \{1, ..., n\}$, α_{ki}, $k = 1, 2$ and α_{ki}^v, $k = 1, 2$ denote the infection rates of a susceptible by contacting respectively an unvaccinated and a vaccinated infected of type k, $k = 1, 2$. Parameters β_i and β_i^v represent respectively the infection rates of a susceptible by contacting an unvaccinated and a vaccinated exposed. Parameters d_{ij}, $j = 1, ..., n$ is the probability that an individual of the j^{th} class infects an individual of the i^{th} one. Parameters q_{ki}, $k = 1, 2$ and q_{ki}^v, $k = 1, 2$ stand for type-k infection rate among the unvaccinated and vaccinated exposed. Parameters r_{1i} and r_{2i} are the removal rates for I_{1i} and I_{2i}, respectively, and δ denotes the probability of infection among vaccinated susceptible.At last, $F_i = \sum_{j=1}^{n}(\alpha_{1i}I_{1j} + \alpha_{2i}I_{2j} + \beta_i E_j + \alpha_{1i}^v I_{1j}^v + \alpha_{2i}^v I_{2j}^v + \beta_i^v E_j^v)d_{ij}$

For analysis purposes, it is useful to put the model into its matrix form which is the following:

$$\begin{cases}
\dot{S} &= -A_1\text{diag}(S)DI_1 - A_2\text{diag}(S)DI_2 - \beta\text{diag}(S)DE - A_1^v\text{diag}(S)DI_1^v \\
&\quad - A_2^v\text{diag}(S)DI_2^v - \beta^v\text{diag}(S)DE^v - \text{diag}(\tau)S \\
\dot{E} &= A_1\text{diag}(S)DI_1 + A_2\text{diag}(S)DI_2 + \beta\text{diag}(S)DE + A_1^v\text{diag}(S)DI_1^v \\
&\quad + A_2^v\text{diag}(S)DI_2^v + \beta^v\text{diag}(S)DE^v - (Q_1 + Q_2)E \\
\dot{I}_1 &= Q_1 E - r_1 I_1 \\
\dot{I}_2 &= Q_2 E - r_2 I_2 \\
\dot{R} &= r_1 I_1 + r_2 I_2 \\
\dot{S}^v &= -\delta A_1\text{diag}(S^v)DI_1 - \delta A_2\text{diag}(S^v)DI_2 - \delta\beta\text{diag}(S^v)DE - \delta A_1^v\text{diag}(S^v)DI_1^v \\
&\quad - \delta A_2^v\text{diag}(S^v)DI_2^v - \delta\beta^v\text{diag}(S^v)DE^v - \text{diag}(\tau)S \\
\dot{E}^v &= \delta A_1\text{diag}(S^v)DI_1 + \delta A_2\text{diag}(S^v)DI_2 + \delta\beta\text{diag}(S^v)DE + \delta A_1^v\text{diag}(S^v)DI_1^v \\
&\quad + \delta A_2^v\text{diag}(S^v)DI_2^v + \delta\beta^v\text{diag}(S^v)DE^v - \left(Q_1^v + Q_2^v\right)E^v \\
\dot{I}_1^v &= Q_1^v E^v - r_1 I_1^v \\
\dot{I}_2^v &= Q_2^v E^v - r_2 I_2^v \\
\dot{R}^v &= r_1 I_1^v + r_2 I_2^v
\end{cases}$$

where, $S = (S_i)_{1\leq i\leq n}$, $E = (E_i)_{1\leq i\leq n}$, $E^v = (E_i^v)_{1\leq i\leq n}$, $I_k = (I_{ki})_{1\leq i\leq n}$, $R = (R_i)_{1\leq i\leq n}$, $S^v = (S_i^v)_{1\leq i\leq n}$, $I_k^v = (I_{ki}^v)_{1\leq i\leq n}$, $R^v = (R_i^v)_{1\leq i\leq n}$, $\tau = (\tau_i)_{1\leq i\leq n}$, $F = (F_i)_{1\leq i\leq n}$, $A_k = \text{diag}\,(\alpha_{1i})_{1\leq i\leq n}$, $A_1^v = \text{diag}\left(\alpha_{1i}^v\right)_{1\leq i\leq n}$, $\beta = \text{diag}\,(\beta_i)_{1\leq i\leq n}$, $\beta^v = \text{diag}\left(\beta_i^v\right)_{1\leq i\leq n}$, $Q_k = \text{diag}\,(q_{ki})_{1\leq i\leq n}$, $Q_k^v = \text{diag}\left(q_{ki}^v\right)_{1\leq i\leq n}$, $r_k = \text{diag}\,(r_{ki})_{1\leq i\leq n}$ and $D = (d_{ij})_{1\leq i,j\leq n}$, for $k = 1, 2$.

Assumptions:

- Let P_i be the population proportion of class i defined as

$$P_i = S_i + E_i + I_{1i} + I_{2i} + S_i^v + E_i^v + I_{1i}^v + I_{2i}^v + R_i + R_i^v.$$

  Each subpopulation, for all $i \in \{1, ..., n\}$, is closed and P_i is constant. Thus, it can be assumed, without loss of generality, that

$$\sum_{i=1}^{n} P_i = 1. \tag{11}$$

- All parameters of the model are considered positive and constant.
- In this study, absence of immunity loss prohibits individuals from removed compartments R_i and R_i^v to return to the susceptible compartments S_i and S_i^v.

3 | ANALYSIS OF THE MODEL WITH CONSTANT CONTROL

In this section, we study the existence of the disease-free equilibrium (DFE) in a particular case where the vaccination rate is supposed constant.

Proposition 1. *The disease-free equilibrium (DFE) of model (1-10), $X^* = (X_1, \ldots, X_n)$ where, for all $i \in \{1, \ldots, n\}$, $X_i = (S_i^*, E_i^*, I_{1i}^*, I_{2i}^*, R_i^*, S_i^{v*}, E_i^{v*}, I_{1i}^{v*}, I_{2i}^{v*}, R_i^{v*})$, is given by:*

- $S_i^* + S_i^v * + R_i^* + R_i^v * = P_i$ *and* $E_i^* = I_{ki}^* = E_i^{v*} = I_{ki}^{v*} = 0$, *if* $\tau_i(t) = 0$.
- $S_i^* = E_i^* = I_{1i}^* = I_{2i}^* = E_i^{v*} = I_{1i}^{v*} = I_{2i}^{v*} = 0$ *and* $S_i^{v*} + R_i^* + R_i^{v*} = P_i$, *if* $\tau_i(t) > 0$.

Proof. For all $i \in \{1, \ldots, \}$, the equilibrium X_i^* is the solution of the following system:

$$\begin{aligned}
0 &= -(F_i + \tau_i)S_i \\
0 &= F_i S_i - (q_{1i} + q_{2i})E_i \\
0 &= q_{1i}E_i - r_{1i}I_{1i} \\
0 &= q_{2i}E_i - r_{2i}I_{2i} \\
0 &= r_{1i}I_{1i} + r_{2i}I_{2i} \\
0 &= \tau_i S_i - \delta F_i S_i^v \\
0 &= \delta F_i S_i^v - (q_{1i}^v + q_{2i}^v)E_i^v \\
0 &= q_{1i}^v E_i^v - r_{1i}I_{1i}^v \\
0 &= q_{2i}^v E_i^v - r_{2i}I_{2i}^v \\
0 &= r_{1i}I_{1i}^v + r_{2i}I_{2i}^v
\end{aligned}$$

According to the first equation of this system, either $S_i = 0$ or $F_i + \tau_i = 0$.

- if $F_i + \tau_i = 0$, then one has $\tau_i = F_i = 0$ which implies that for all $j \in \{1, \ldots, n\}, I$

  $E_j = E_j^v = I_{kj} = I_{kj}^v = 0, \forall j \in \{1, \ldots, n\}$ and $k \in \{1, 2\}$
  $R_i = R_i^0$ and $R_i = R_i^{v0}$
  $S_i = S_i^0$ and $S_i^v = S_i^{v0}$ such that $S_i^0 + S_i^{v0} + R_i^0 + R_i^{v0}) = P_i$

- if $S_i = 0$, then one has $F_i + \tau_i \geq 0$

$S_i = E_i = E_i^v = I_{ki} = I_{ki}^v = 0, k \in \{1, 2\}$
$R_i = R_i^0$ and $R_i = R_i^{v0}$
$S_i^v = S_i^v(0)$ such that $S_i^{v0} + R_i^0 + R_i^{v0} = P_i$

Thus, for all $i \in \{1, \ldots, n\}$, an equilibrium point X_i^* of age class i, has one of the following forms

TABLE 1 This is sample table caption.

If $\tau_i = 0$		**If** $\tau_i > 0$
$X_i^* = (P_i, 0, 0, 0, 0, 0, 0, 0, 0, 0)$	$X_i^* = (S_i^0, 0, 0, 0, 0, 0, 0, 0, 0, R_i^{v0})$	$X_i^* = (0, 0, 0, 0, P_i, 0, 0, 0, 0, 0)$
$X_i^* = (0, 0, 0, 0, P_i, 0, 0, 0, 0, 0)$	$X_i^* = (0, 0, 0, 0, R_i^0, S_i^{v0}, 0, 0, 0, 0)$	$X_i^* = (0, 0, 0, 0, 0, P_i, 0, 0, 0, 0)$
$X_i^* = (0, 0, 0, 0, 0, P_i, 0, 0, 0, 0)$	$X_i^* = (0, 0, 0, 0, 0, S_i^{v0}, 0, 0, 0, R_i^{v0})$	$X_i^* = (0, 0, 0, 0, 0, 0, 0, 0, 0, P_i)$
$X_i^* = (0, 0, 0, 0, 0, 0, 0, 0, 0, P_i)$	$X_i^* = (S_i^0, 0, 0, 0, R_i^0, 0, 0, 0, 0, R_i^{v0})$	$X_i^* = (0, 0, 0, 0, R_i^0, S_i^{v0}, 0, 0, 0, 0)$
$X_i^* = (S_i^0, 0, 0, 0, 0, S_i^{v0}, 0, 0, 0, 0)$	$X_i^* = (S_i^0, 0, 0, 0, R_i^0, S_i^{v0}, 0, 0, 0, 0)$	$X_i^* = (0, 0, 0, 0, R_i^0, 0, 0, 0, 0, R_i^{v0})$
$X_i^* = (0, 0, 0, 0, R_i^0, 0, 0, 0, 0, R_i^{v0})$	$X_i^* = (0, 0, 0, 0, R_i^0, S_i^{v0}, 0, 0, 0, R_i^{v0})$	$X_i^* = (0, 0, 0, 0, 0, S_i^{v0}, 0, 0, 0, R_i^{v0})$
$X_i^* = (S_i^0, 0, 0, 0, R_i^0, 0, 0, 0, 0, 0)$	$X_i^* = (S_i^0, 0, 0, 0, 0, S_i^{v0}, 0, 0, 0, R_i^{v0})$	$X_i^* = (0, 0, 0, 0, R_i^0, S_i^{v0}, 0, 0, 0, R_i^{v0})$

□

To construct the next-generation matrix, only equations corresponding to the infectious compartments are considered, i.e. (2), (3), (4), (7), (8) and (9), for all age groups.

Proposition 2. *The basic reproduction number R_0 is strictly positive and corresponds to the dominant eigenvalue of the matrix*

$$\tilde{M} = M_1(Q_1 + Q_2)^{-1}$$

where

- $P = (P_1, \ldots, P_n)$
- $M_1 = \left(\beta \text{diag}(P)D + A_1 \text{diag}(P)Dr_1^{-1}Q_1 + A_2 \text{diag}(P)Dr_2^{-1}Q_2\right)$

Proof. The basic reproduction number R_0 is related to the start of the epidemy as it allows the measurement of the secondary cases of infection caused by one infected individual introduced to a population of susceptible individuals. Thus, in order to compute it, the next-generation matrix is evaluated at disease-free equilibrium $X = (X_i)_{1 \leq i \leq n}$ where $X_i = (P_i, 0, \ldots, 0)$ for all $i \in \{1, \ldots, n\}$ with the assumption of vaccination absence i.e.$\tau_i = 0$ for all $i \in \{1, \ldots, n\}$. The non-negative matrix, F, corresponding to the new infections in the population, evaluated at the disease-free equilibrium $X^* = (X_i^*)_{1 \leq i \leq n} = (P_i, 0, 0, 0, 0, 0, 0, 0, 0, 0)_{1 \leq i \leq n}$, is given by:

$$\mathrm{F} = \left(\begin{array}{ccc|ccc} \beta \text{diag}(S)D & A_1 \text{diag}(S)D & A_2 \text{diag}(S)D & \beta^v \text{diag}(S)D & A_1^v \text{diag}(S)D & A_2^v \text{diag}(S)D \\ 0 & 0 & 0 & 0 & 0 & 0 \\ 0 & 0 & 0 & 0 & 0 & 0 \\ \hline 0 & 0 & 0 & 0 & 0 & 0 \\ 0 & 0 & 0 & 0 & 0 & 0 \\ 0 & 0 & 0 & 0 & 0 & 0 \end{array}\right) = \begin{pmatrix} F_1 & F_2 \\ 0 & 0 \end{pmatrix}$$

The non-singular matrix, V, corresponding to the transfer of individuals in and out of compartments, is:

$$\mathrm{V} = \left(\begin{array}{ccc|ccc} -(Q_1+Q_2) & 0 & 0 & 0 & 0 & 0 \\ Q_1 & -r_1 & 0 & 0 & 0 & 0 \\ Q_2 & 0 & -r_2 & 0 & 0 & 0 \\ \hline 0 & 0 & 0 & -(Q_1^v+Q_2^v) & 0 & 0 \\ 0 & 0 & 0 & Q_1^v & -r_1 & 0 \\ 0 & 0 & 0 & Q_2^v & 0 & -r_2 \end{array}\right) = \begin{pmatrix} V_1 & 0 \\ O & V_2 \end{pmatrix}$$

Then,

$$\mathrm{V}^{-1} = \begin{pmatrix} V_1^{-1} & 0 \\ O & V_2^{-1} \end{pmatrix}$$

where,

$$\mathrm{V}_1^{-1} = \begin{pmatrix} -(Q_1+Q_2)^{-1} & 0 & 0 \\ -r_1^{-1}Q_1(Q_1+Q_2)^{-1} & -r_1^{-1} & 0 \\ -r_2^{-1}Q_2(Q_1+Q_2)^{-1} & 0 & -r_2^{-1} \end{pmatrix} \quad \text{and} \quad \mathrm{V}_2^{-1} = \begin{pmatrix} -(Q_1^v+Q_2^v)^{-1} & 0 & 0 \\ -r_1^{-1}Q_1^v(Q_1^v+Q_2^v)^{-1} & -r_1^{-1} & 0 \\ -r_2^{-1}Q_2^v(Q_1^v+Q_2^v)^{-1} & 0 & -r_2^{-1} \end{pmatrix}$$

The basic reproduction number, R_0, corresponds to the dominant eigenvalue of the next generation matrix M, defined as follows:

$$\mathrm{M} = -\mathrm{F}\mathrm{V}^{-1} = \begin{pmatrix} -F_1V_1^{-1} & -F_2V_2^{-1} \\ 0 & 0 \end{pmatrix}$$

where,

$$-\mathrm{F}_1\mathrm{V}_1^{-1} = \begin{pmatrix} M_1(Q_1+Q_2)^{-1} & A_1\mathrm{diag}(S)Dr_1^{-1} & A_2\mathrm{diag}(S)Dr_2^{-1} \\ 0 & 0 & 0 \\ 0 & 0 & 0 \end{pmatrix} \quad \text{and} \quad -\mathrm{F}_2\mathrm{V}_2^{-1} = \begin{pmatrix} M_2(Q_1^v+Q_2^v)^{-1} & A_1^v\mathrm{diag}(S)Dr_1^{-1} & A_2^v\mathrm{diag}(S)Dr_2^{-1} \\ 0 & 0 & 0 \\ 0 & 0 & 0 \end{pmatrix}$$

where M_1 and M_2 are defined as follows:

$$M_1 = \left(\beta\mathrm{diag}(S)D + A_1\mathrm{diag}(S)Dr_1^{-1}Q_1 + A_2\mathrm{diag}(S)Dr_2^{-1}Q_2\right)$$

$$M_2 = \left(\beta^v\mathrm{diag}(S)D + A_1^v\mathrm{diag}(S)Dr_1^{-1}Q_1^v + A_2^v\mathrm{diag}(S)Dr_2^{-1}Q_2^v\right)$$

Thus, the basic reproduction number corresponds to the dominant eigenvalue of the next-generation matrix M given by:

$$\mathrm{M} = \begin{pmatrix} M_1(Q_1+Q_2)^{-1} & A_1\mathrm{diag}(P)Dr_1^{-1} & A_2\mathrm{diag}(P)Dr_2^{-1} & M_2(Q_1^v+Q_2^v)^{-1} & A_1^v\mathrm{diag}(P)Dr_1^{-1} & A_2^v\mathrm{diag}(P)Dr_2^{-1} \\ 0 & 0 & 0 & 0 & 0 & 0 \\ \vdots & \vdots & \vdots & \vdots & \vdots & \vdots \\ 0 & 0 & 0 & 0 & 0 & 0 \end{pmatrix}$$

The characteristic polynomial of M is given by:

$$P_M(\lambda) = (-\lambda)^{5n}.det(M_1.(Q_1+Q_2)^{-1} - \lambda I_n)$$

Let $\tilde{M}$ be the matrix defined by:

$$\tilde{M} = M_1.(Q_1+Q_2)^{-1}$$

Hence, other then 0, P_M has the same roots as $P_{\tilde{M}} = det(M_1.(Q_1+Q_2)^{-1} - \lambda I_n)$. Assuming that all parameters of the model are strictly positive as well as P_i for all $i \in \{1,\ldots,n\}$, then, one can say that $\tilde{M}$ has strictly positive coefficients and is consequently irreducible. Hence according to the theorem of Perron-Frobenius, ρ, the dominant eigenvalue of $\tilde{M}$, is a simple eigenvalue. Moreover, one has

$$s \leq \rho \leq S$$

where $s = \min_{1\leq i\leq n} S_i$, $S = \max_{1\leq i\leq n} S_i$ and $S_i = \sum_{j=1}^{n} \frac{p_j d_{ij}}{q_{1j}+q_{2j}} \left(\beta_i + \alpha_{1i}\frac{q_{1j}}{r_{1j}} + \alpha_{2i}\frac{q_{2j}}{r_{2j}}\right)$.

And since all parameters are strictly positive, then so is s which implies that $\rho > 0$. Consequently, as R_0 corresponds to the spectral radius of M, then $R_0 = \rho$.

□

4 | OPTIMAL CONTROL PROBLEM

The present section is devoted to ascertaining the optimal vaccination strategy under different scenarios. A good vaccination strategy is evaluated in terms of its impact on the proportion of severely infected individuals in both the vaccinated and unvaccinated subgroups. The optimal strategy is the one that minimizes the number of critical cases (ones that need hospitalization) over the whole period $[0, T]$ where the control is the vector of vaccination rates $0 \leq \tau_i(t) \leq \tau_i^{max}$ where τ_i^{max} represents the maximal vaccination rate and 0 represents the minimal one which stands for no vaccination at all.

The objective of this study is to determine the optimal vaccination strategy that minimizes the number of critical cases among the vaccinated and the unvaccinated I_2 and I_2^v. Thus, for all t in $[0, T]$, the Lagrangian L is defined as follows:

$$L(I_2, I_2^v) = \sum_{i=1}^{n} I_{2i}^2(t) + I_{2i}^{v2}(t)$$

Thus, the optimal control problem is given by:

$$\min_{0\leq\tau\leq\tau_i^{max}} \int_0^T L(t)dt \tag{12}$$

subject to the system (1-10).

Let U be the set of admissible controls given by:

$$U = \{\tau(t) = (\tau_i(t))_{1\leq i\leq n}, \forall 1 \leq i \leq n, \tau_i(t) \in L^1([0, \tau_i^{max}])\}$$

Proposition 3. *There exists an optimal control* $\tau^* = (\tau_i^*)_{1\leq i\leq n}$ *and a corresponding state variables vector* $\left(S_i, E_i, I_{1i}, I_{2i}, R_i, S_i^v, E_i^{v0}, I_{1i}^v, I_{2i}^v, R_i^v\right)_{1\leq i\leq n}$ *that minimizes the objective function.*

Proof. The existence of the optimal control pair can be obtained using a result by [12,21].
In fact, one can easily verify that:

1. For $\tau_i = 0$, there exists a corresponding solution to the model according to Cauchy-Lipschitz theorem. Thus the set of controls and corresponding state variables is nonempty.
2. Let $\tau^1, \tau^2 \in U$ and $\psi \in [0, 1]$. Then one has $\psi\tau^1 + (1-\psi)\tau^2 \in U$.
   Moreover, for a sequence $(\tau^p) \subset U$ such that $\lim_{p\to+\infty} \tau^p = \tau$, one has $\tau \in U$.
   Hence, the admissible set of controls is convex and closed.
3. The right-hand side of the state system (1-10, 12) is bounded by a linear function in the state and control variables. In fact, for all $i \in \{1, \ldots, n\}$ and for $k \in \{1, 2\}$, one has

$$|\dot{S}_i| \leq max(\alpha_{ki}, \beta_{ki}, \alpha_{ki}^v, \beta_{ki}^v)\|X\| + \|\tau\|$$

$$|\dot{E}_i| \leq (max(\alpha_{ki}, \beta_{ki}, \alpha_{ki}^v, \beta_{ki}^v) + q_{1i} + q_{2i})\|X\| + \|\tau\|$$

$$|\dot{I}_{ki}| \leq (q_{ki} + r_{ki})\|X\| + \|\tau\|$$

$$|\dot{R}_i| \leq (r_{1i} + r_{2i})\|X\| + \|\tau\|$$

$$|\dot{S}_i^v| \leq \delta\, max(\alpha_{ki}, \beta_{ki}, \alpha_{ki}^v, \beta_{ki}^v)\|X\| + \|\tau\|$$

$$|\dot{E}_i| \leq (\delta\, max(\alpha_{ki}, \beta_{ki}, \alpha_{ki}^v, \beta_{ki}^v) + q_{1i}^v + q_{2i}^v)\|X\| + \|\tau\|$$

$$|\dot{I}_{ki}| \leq (q_{ki}^v + r_{ki})\|X\| + \|\tau\|$$

$$|\dot{R}_i| \leq (r_{1i} + r_{2i})\|X\| + \|\tau\|$$

4. The integrand of the objective functional L is convex on U since its constant in τ.
5. Since $L \geq 0$. We consider treating the cases $L = 0$ For $L > 0$, there exist constants $\omega_1 > 0, \omega_2 > 0$ and $\rho > 1$ such that

$$L \geq \omega_2 + \omega_1 (\sum_{k=1}^{n} \tau_k^2)^{\frac{\rho}{2}}$$

where $\omega_1 = \frac{\epsilon}{2\sqrt{n}\tau_{max}}$, $\omega_2 = \frac{\epsilon}{2}$, $\rho = 2$ and $\epsilon = \left(\sum_{i=1}^{n} I_{2i}^2(0) + I_{2i}^{v2}(0) \right) e^{-r_{2i}T}$ In fact, one has:

$$I_{2i}(t) = \left(I_{2i}(0) + q_{2i} \int_0^t E_i(s) e^{r_{2i}s} ds \right) e^{-r_{2i}t}$$

$$I_{2i}^v(t) = \left(I_{2i}^v(0) + q_{2i}^v \int_0^t E_i(s) e^{r_{2i}s} ds \right) e^{-r_{2i}t}$$

Thus,

$$I_{2i}^2(t) = \left(I_{2i}^2(0) + 2I_{2i}(0) q_{2i} \int_0^t E_i(s) e^{r_{2i}s} + q_{2i}^2 \left(\int_0^t E_i(s) e^{r_{2i}s} ds \right)^2 \right) e^{-2r_{2i}t}$$

$$I_{2i}^{v2}(t) = \left(I_{2i}^{v2}(0) + 2I_{2i}^v(0) q_{2i}^v \int_0^t E_i(s) e^{r_{2i}s} + q_{2i}^{v2} \left(\int_0^t E_i(s) e^{r_{2i}s} ds \right)^2 \right) e^{-2r_{2i}t}$$

Since all the sum terms are positive, one can say that

$$L \geq \sum_{i=1}^{n} \left(I_{2i}^2(0) + I_{2i}^{v2}(0) \right) e^{-2r_{2i}T}$$

Let $\epsilon = \sum_{i=1}^{n} \left(I_{2i}^2(0) + I_{2i}^{v2}(0) \right) e^{-2r_{2i}T}$, then one has

$$\epsilon = \frac{\epsilon}{2\|\tau\|^2} \|\tau\|^2 + \frac{\epsilon}{2} \geq \frac{\epsilon}{2\sqrt{n}\tau_{max}} \|\tau\|^2 + \frac{\epsilon}{2}$$

□

In order to determine the optimal control, Pontryagin's Minimum Principle was used[21].
The Hamiltonian is given by:

$$H(t, \tau, X, \lambda) = \langle \lambda(t), \dot{X}(t) \rangle + \sum_{i=1}^{n} I_{2i}^2 + I_{2i}^{v2}$$

where $X = (X_i)_{1 \leq i \leq n}$ is the vector of state variables previously defined and $\lambda = (\lambda_i)_{1 \leq i \leq n}$ is the vector of adjoint variables with

$$\lambda_i = (\lambda_{S_i}(t), \lambda_{E_i}(t), \lambda_{I_{1i}}(t), \lambda_{I_{2i}}(t), \lambda_{R_i}(t), \lambda_{S_i^v}(t), \lambda_{E_i^v}(t), \lambda_{I_{1i}^v}(t), \lambda_{I_{2i}^v}(t), \lambda_{R_i^v}(t))$$

and $\langle ., . \rangle$ is the scalar product.

Proposition 4. *Given optimal controls $\tau_1^*, \ldots, \tau_n^*$ and the corresponding solution $X(t)$ of the corresponding state system (1-10) - (12), there exists a vector of adjoint variables $\lambda = (\lambda_i)_{1 \leq i \leq n}$ that satisfy:*

$$\dot{\lambda_{S_i}} = (F_i + \tau_i)\lambda_{S_i} - F_i\lambda_{E_i} - \tau_i\lambda_{S_i^v} \tag{13}$$

$$\dot{\lambda_{E_i}} = \sum_{j=1}^{n} \beta_j d_{ji} \left(S_j(\lambda_{S_j} - \lambda_{E_j}) + \delta\, S_j^v(\lambda_{S_j^v} - \lambda_{E_j^v}) \right) + (q_{1i} + q_{2i})\lambda_{E_i} - q_{1i}\lambda_{I_{1i}} - q_{2i}\lambda_{I_{2i}} \tag{14}$$

$$\dot{\lambda_{I_{1i}}} = \sum_{j=1}^{n} \alpha_{1j} d_{ji} \left(S_j(\lambda_{S_j} - \lambda_{E_j}) + \delta\, S_j^v(\lambda_{S_j^v} - \lambda_{E_j^v}) \right) + r_{1i}\lambda_{I_{1i}} \tag{15}$$

$$\dot{\lambda_{I_{2i}}} = \sum_{j=1}^{n} \alpha_{2j} d_{ji} \left(S_j(\lambda_{S_j} - \lambda_{E_j}) + \delta\, S_j^v(\lambda_{S_j^v} - \lambda_{E_j^v}) \right) + r_{2i}\lambda_{I_{1i}} - 2I_{2i} \tag{16}$$

$$\dot{\lambda_{R_i}} = 0 \tag{17}$$

$$\dot{\lambda_{S_i^v}} = \delta\, F_i(\lambda_{S_i^v} - \lambda_{E_i^v}) \tag{18}$$

$$\dot{\lambda_{E_i^v}} = \sum_{j=1}^{n} \beta_j^v d_{ji} \left(S_j(\lambda_{S_j} - \lambda_{E_j}) + \delta S_j^v(\lambda_{S_j^v} - \lambda_{E_j^v}) \right) + (q_{1i}^v + q_{2i}^v)\lambda_{E_i}^v - q_{1i}^v\lambda_{I_{1i}^v} - q_{2i}^{\lambda} I_{2i} \tag{19}$$

$$\dot{\lambda_{I_{1i}^v}} = \sum_{j=1}^{n} \alpha_{1j}^v d_{ji} \left(S_j(\lambda_{S_j} - \lambda_{E_j}) + \delta\, S_j^v(\lambda_{S_j^v} - \lambda_{E_j^v}) \right) + r_{1i}\lambda_{I_{1i}} \tag{20}$$

$$\dot{\lambda_{I_{2i}^v}} = \sum_{j=1}^{n} \alpha_{2j}^v d_{ji} \left(S_j(\lambda_{S_j} - \lambda_{E_j}) + \delta\, S_j^v(\lambda_{S_j^v} - \lambda_{E_j^v}) \right) + r_{2i}\lambda_{I_{1i}} - 2I_{2i} \tag{21}$$

$$\dot{\lambda_{R_i}^v} = 0 \tag{22}$$

with transversality conditions:

$$\lambda(T) = 0. \tag{23}$$

Furthermore, the optimal control is given by $\tau^* = (\tau_1^*, \ldots, \tau_n^*)$ *where for all* $i \in \{1, \ldots, n\}$,

$$\tau_i^* = \begin{cases} 0 & , \text{if } \lambda_{S_i^v} S_i^v - \lambda_{S_i} S_i > 0 \\ \tau_i^{max} & , \text{if } \lambda_{S_i^v} S_i^v - \lambda_{S_i} S_i < 0 \\ \text{singular} & , \text{if } \lambda_{S_i^v} S_i^v - \lambda_{S_i} S_i = 0 \end{cases}$$

Proof. According to Pontryagin's minimum principle, for all $i \in \{1, \dots, n\}$ the adjoint variables satisfy:

$$
\begin{aligned}
\dot{\lambda}_{S_i} &= -\frac{\partial H}{\partial S_i} = (F_i + \tau_i)\lambda_{S_i} - F_i\lambda_{E_i} - \tau_i\lambda_{S_i^v} \\
\dot{\lambda}_{E_i} &= -\frac{\partial H}{\partial E_i} = \sum_{j=1}^{n} \beta_j d_{ji} S_j(\lambda_{S_j} - \lambda_{E_j}) + \delta \sum_{j=1}^{n} \beta_j d_{ji} S_j^v(\lambda_{S_j^v} - \lambda_{E_j^v}) + (q_{1i} + q_{2i})\lambda_{E_i} - q_{1i}\lambda_{I_{1i}} - q_{2i}\lambda_{I_{2i}} \\
\dot{\lambda}_{I_{1i}} &= -\frac{\partial H}{\partial I_{1i}} = \sum_{j=1}^{n} \alpha_{1j} d_{ji} S_j(\lambda_{S_j} - \lambda_{E_j}) + \delta \sum_{j=1}^{n} \alpha_{1j} d_{ji} S_j^v(\lambda_{S_j^v} - \lambda_{E_j^v}) + r_{1i}(\lambda_{I_{1i}} - \lambda_{R_i}) \\
\dot{\lambda}_{I_{2i}} &= -\frac{\partial H}{\partial I_{2i}} = \sum_{j=1}^{n} \alpha_{2j} d_{ji} S_j(\lambda_{S_j} - \lambda_{E_j}) + \delta \sum_{j=1}^{n} \alpha_{2j} d_{ji} S_j^v(\lambda_{S_j^v} - \lambda_{E_j^v}) + r_{2i}(\lambda_{I_{1i}} - \lambda_{R_i}) - 2I_{2i} \\
\dot{\lambda}_{R_i} &= -\frac{\partial H}{\partial R_i} = 0 \\
\dot{\lambda}_{S_i^v} &= -\frac{\partial H}{\partial S_i^v} = \delta F_i(\lambda_{S_i^v} - \lambda_{E_i^v}) \\
\dot{\lambda}_{E_i^v} &= -\frac{\partial H}{\partial E_i^v} = \sum_{j=1}^{n} \beta_j^v d_{ji} S_j(\lambda_{S_j} - \lambda_{E_j}) + \delta \sum_{j=1}^{n} \beta_j^v d_{ji} S_j^v(\lambda_{S_j^v} - \lambda_{E_j^v}) + (q_{1i}^v + q_{2i}^v)\lambda_{E_i}^v - q_{1i}^v\lambda_{I_{1i}^v} - q_{2i}^{\lambda} I_{2i} \\
\dot{\lambda}_{I_{1i}^v} &= -\frac{\partial H}{\partial I_{1i}^v} = \sum_{j=1}^{n} \alpha_{1j}^v d_{ji} S_j(\lambda_{S_j} - \lambda_{E_j}) + \delta \sum_{j=1}^{n} \alpha_{1j}^v d_{ji} S_j^v(\lambda_{S_j^v} - \lambda_{E_j^v}) + r_{1i}(\lambda_{I_{1i}} - \lambda_{R_i}^v) \\
\dot{\lambda}_{I_{2i}^v} &= -\frac{\partial H}{\partial I_{2i}^v} = \sum_{j=1}^{n} \alpha_{2j}^v d_{ji} S_j(\lambda_{S_j} - \lambda_{E_j}) + \delta \sum_{j=1}^{n} \alpha_{2j}^v d_{ji} S_j^v(\lambda_{S_j^v} - \lambda_{E_j^v}) + r_{2i}(\lambda_{I_{1i}} - \lambda_{R_i}^v) - 2I_{2i} \\
\dot{\lambda}_{R_i}^v &= -\frac{\partial H}{\partial R_i^v} = 0
\end{aligned}
$$

with the final conditions

$$\lambda_i(t^f) = 0$$

Moreover, the Pontryagin's Minimum Principle states that the optimal control τ^* minimizes the Hamiltonian, hence we should seek the minimum of H with respect to τ_i, $i \in \{1, ..., n\}$. Since

$$\frac{\partial H}{\partial \tau_i} = \lambda_{S_i^v} S_i^v - \lambda_{S_i} S_i,$$

the minimum is either reached at $\tau_i^* = 0$ or $\tau_i^* = \tau_i^{max}$ according to the sign of $\lambda_{S_i^v} S_i^v - \lambda_{S_i} S_i$.
However, if there exists an interval $[t_0; t_1] \subset [0; T]$, such that the switching function $\lambda_{S_i^v}(t) S_i^v(t) - \lambda_{S_i}(t) S_i(t) = 0$, for all $t \in [t_0; t_1]$ the control is considered singular. □

5 | NUMERICAL SIMULATIONS AND DISCUSSION

In this section, we conduct numerical simulations using parameters of Covid-19. In order to simulate the optimal control corresponding to the various age distributions, we use data of three countries presenting the main three different age distributions: expansive (Senegal), Stationary (Tunisia) and Constrictive (USA)(See table A1).

The problem was solved using the Python optimization suite GEKKO [†] [20]. During all the simulation process, the populations studied were divided into six age groups: 0 – 14 years(class 1) , 15 – 29 years (class 2), 30 – 44 years (class 3), 45 – 59 years (class 4), 60, 74 years (class 5) and $\geq$ 75 years (class 6) [‡].

Moreover, Covid-19 high sensitivity to the age of the individuals among the population studied sets the ground for certain questions to arise about the effect that different age distributions can have on the optimal strategy that is to be chosen.

[†] https://github.com/BYU-PRISM/GEKKO
[‡] https://covid19.who.int/WHO-COVID-19-global-data.csv

TABLE 2 Different types of age pyramids.

Expansive: young and growing	Stationary:non growing	Constrictive:elderly and shrinking
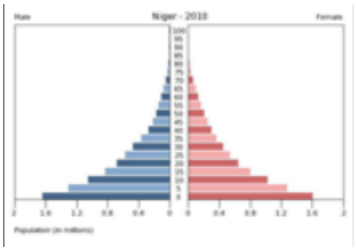	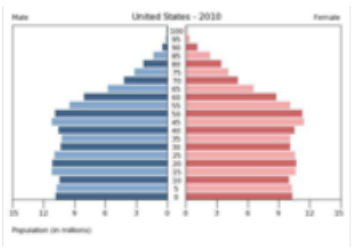	

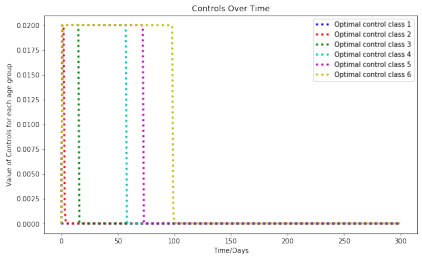

(a) Optimal vaccination for stationary age distribution with 25% maximal threshold

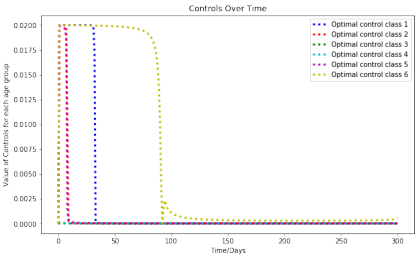

(b) Optimal vaccination for expansive age distribution with 25% maximal threshold

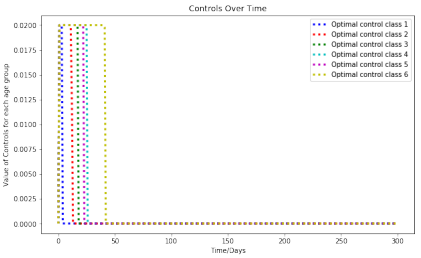

(c) Optimal vaccination for constrictive age distribution with 25% maximal threshold

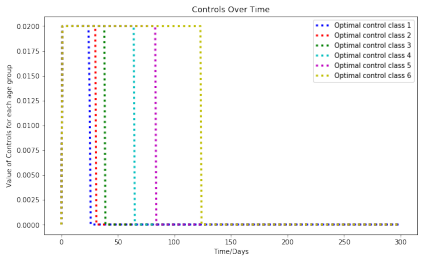

(d) Optimal vaccination for stationary age distribution with 50% maximal threshold

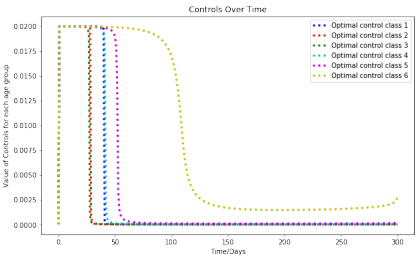

(e) Optimal vaccination for expansive age distribution with 50% maximal threshold

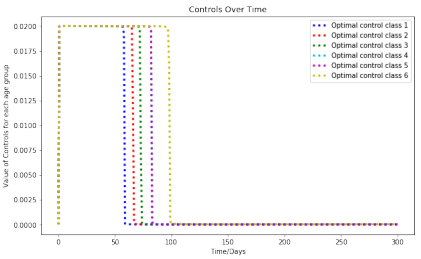

(f) Optimal vaccination for constrictive age distribution with 50% maximal threshold

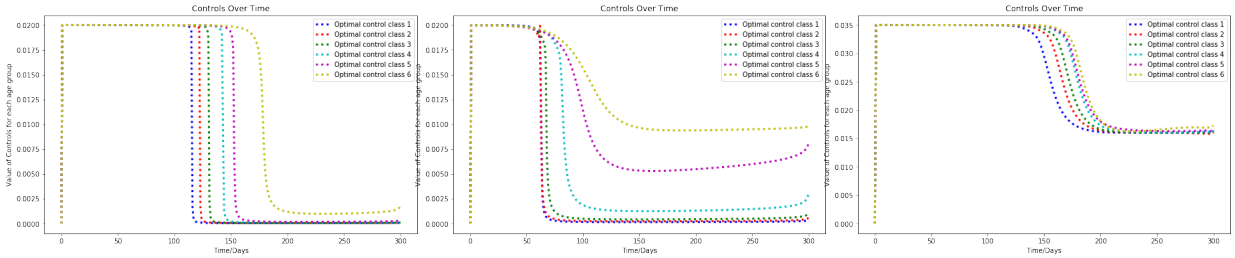

(g) Optimal vaccination for stationary age distribution with 75% maximal threshold (h) Optimal vaccination for expansive age distribution with 75% maximal threshold (i) Optimal vaccination for constrictive age distribution with 75% maximal threshold

FIGURE 2 Optimal vaccination for different age distributions: stationary((a), (d) and(g)), expansive ((b), (e) and (h)) and constrictive((c), (f) and (i)) three different maximal vaccination thresholds: 25%, 50% and 75% of the total population

Thereafter, we conducted the simulations using data of three countries exhibiting different age distributions with the objective of determining the optimal vaccination strategy for each country [22]. And as one of the major limitations that faced many countries at the start was the vaccine shortage, we tried to take that into account by setting three different maximal thresholds of vaccination. In the first case, it is assumed that the vaccine availability allows for only 25% of the total population to be vaccinated. In the second case, the maximal vaccination threshold is set at 50%. At last, it is assumed that it is possible to provide vaccination up until 75% of the total size of the population. The results are then, compared to the vaccination strategy set by the WHO. This strategy is composed of several successive steps. The first step consists of vaccinating the oldest class and the at-high-risk

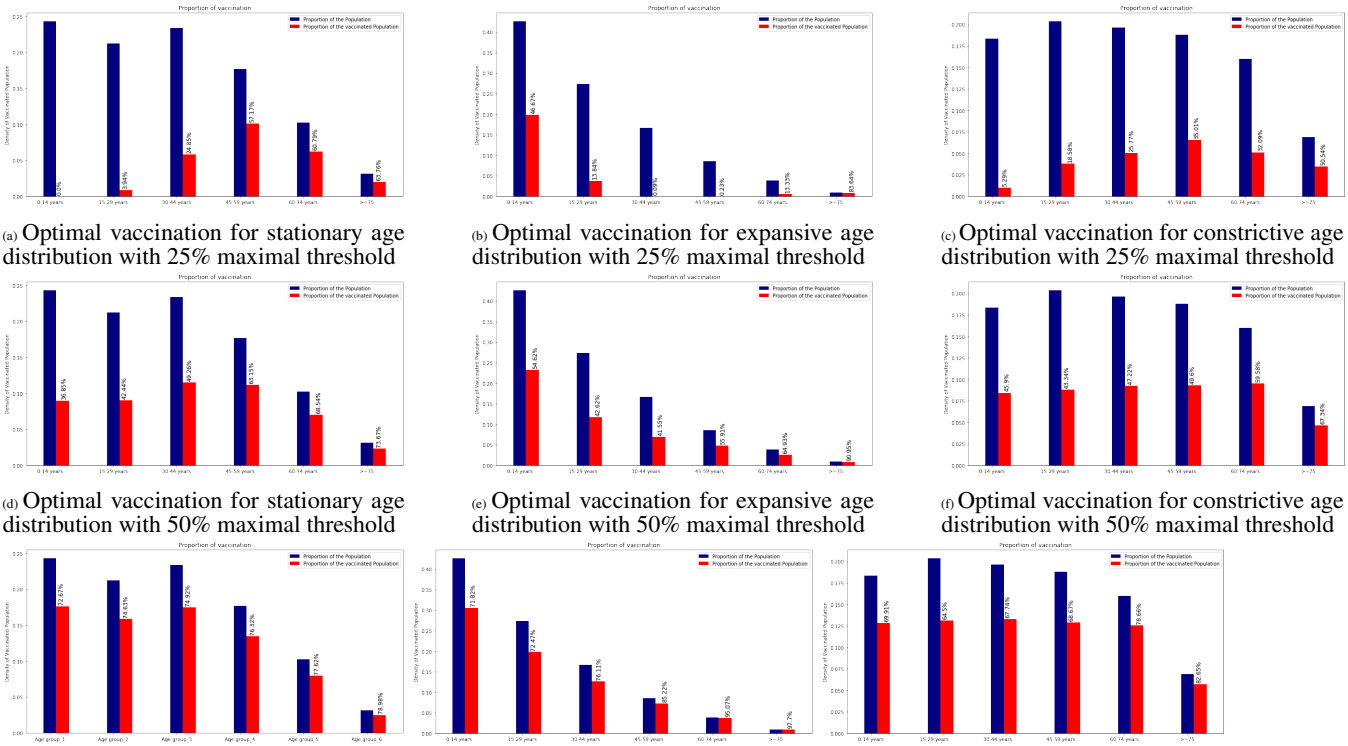

(a) Optimal vaccination for stationary age distribution with 25% maximal threshold

(b) Optimal vaccination for expansive age distribution with 25% maximal threshold

(c) Optimal vaccination for constrictive age distribution with 25% maximal threshold

(d) Optimal vaccination for stationary age distribution with 50% maximal threshold

(e) Optimal vaccination for expansive age distribution with 50% maximal threshold

(f) Optimal vaccination for constrictive age distribution with 50% maximal threshold

(g) Optimal vaccination for stationary age distribution with 75% maximal threshold

(h) Optimal vaccination for expansive age distribution with 75% maximal threshold

(i) Optimal vaccination for constrictive age distribution with 75% maximal threshold

FIGURE 3 Vaccinated proportion of each age class according to the optimal vaccination rate for different age distributions: stationary((a), (d) and(g)), expansive ((b), (e) and (h)) and constrictive((c), (f) and (i)) three different maximal vaccination thresholds: 25%, 50% and 75% of the total population

groups such as health workers. At the end of this step, and if there are still vaccines available, the second step is triggered. This step consists of moving to the next-in-age class and the iterative process then continues until the end of the vaccine stocks in availability.

As a matter of fact, a major difference from the WHO vaccination strategy is noticed for all maximal vaccination thresholds. This difference corresponds to the simultaneous vaccination of all age groups no matter how tight or loose the constraint of vaccine availability is. When maximal vaccination threshold is set to 25% of the total population, one notices for the stationary case that the optimal strategy is more inclined to prioritize the old despite the simultaneous administration of the vaccine to all the age classes. For the expansive distribution, the optimal strategy prioritizes the two oldest classes and the two youngest ones. And taking the USA, one obtains a more or less equal distribution among all the age classes in the population. Clearly, the optimal distributions are not similar, yet one common aspect can be noticed among them which is prioritization according to both age and proportion among the population. This aspect is most clear for the expansive distribution in the first place, then the constrictive case. And although it does not seem to apply in the case of the stationary distribution, attentive observation reveals that it does as most of the individuals belong to one of the four oldest classes. However, once the constraint of the maximal vaccination threshold is set high enough, the optimal strategies of the different age distributions start converging towards a more similar behavior where the oldest classes are prioritized while other classes show close vaccination proportions. This only puts emphasis on the fact that priority is accorded based on the proportion of the class among the population as much as it is based on age . The similarity then tends to be even more visible when the maximal threshold is set to 75% (See figures 2 and 3). As a matter of fact, the loose constraint allows more equal distribution due to easy access to the vaccine. This tendency to show the same shape as the age pyramid is actually a result of the loose constraints that erase the urge to prioritize based on age. The impact of age is quite visible when coupled with tight constraints. In fact, despite the shortage of vaccines, the optimal vaccination strategy is based on similar vaccination of all age classes right from the start of the campaign. On the opposite, the WHO vaccination strategy is based on a successive age-prioritization-based approach based on successive vaccination of different classes. In fact, the optimal control strategy suggests simultaneous vaccination of all the classes while the WHO strategy implies moving to the young

classes only when the old ones are completely vaccinated which can result in not vaccinating young individuals when vaccines are constrained to low maximal thresholds. Moreover, according to the optimal vaccination, the prioritization depends on both the age of the individuals and the age distribution among the population. Whereas, the WHO strategy prioritization is based only on the individuals'age. Additionally, the optimal strategy has a tendency to mimic the age distribution of the population rather than have a uniform behavior that does not depend on the population's age. However, the results of the simulations can be improved by improving the model itself. In fact, the absence of immunity loss is a limitation of the model that does not allow to conduct a long-term study of the optimal vaccination and limits all the results to no more than a six-month time interval. As a perspective, we suggest conducting this study over a longer period of time adding immunity loss for optimizing long-term vaccination strategy as well as vaccination to different non vaccinated compartments other then the infected ones.

6 | CONCLUSION

In this work, an age-structured SEIR mathematical model for infectious disease spread is developed. Then an optimal control problem that aims to determine the vaccination strategy that minimizes critical infections, with vaccination rate as the control, is developed and studied. The steady states were determined under the assumption of constant control along with the the basic reproduction number.

The model was simulated for the ongoing Covid-19 pandemic using parameters that were estimated based on real data of the daily confirmed cases of countries presenting three different age distributions: Tunisia, Senegal, and USA. For the three age distributions, the optimal strategy was checked under different constraints: vaccination ability respectively limited to 25%, 50%, and 75% of the total population. The simulations revealed a number of differences and similarities with the WHO vaccination strategy. In fact, the optimal strategy is unique as it follows the age distribution of the population studied. The results suggest to start vaccinating all age groups at the same time, no matter what the present constraint is. The vaccination duration, however, differs from one class to the other and according to the constraints.

The results of this study do not imply by any means that countries should aim for less than 100% of population vaccination against any infectious disease. It merely presents an alternative for countries that can not achieve such an objective for any reason.

To sum up, one can say that there is no optimal strategy that works for all different countries. Optimal strategy is affected by several factors such as the population mean age and contact matrix. However, all strategies intersect when it comes to prioritizing the oldest age group. The optimal strategy also requires prioritizing the mass regardless of their age. This is a response to the age distribution and the contact matrix impact. And it is explained by several reasons mostly related to their important proportion among the total population as well as their wide contact webs that can badly affect certain vital parameters such as the transmission rate of the disease.

How to cite this article: Bouhali A., Ben Aribi W., Ben Miled S., and Kebir A. Age-optimal vaccination strategy for respiratory infectious disease: a constraint-dependant approach *Mathematical Methods in The Applied Sciences* .

APPENDIX

A APPENDIX

Most parameters used were either taken from literature or estimated based on real data. In fact, the estimation of the basic reproduction number based on data from March 2021 resulted in $R_0 = 2.19$. The infection rates by unvaccinated type-1 infected α_{1i}, $1 \leq i \leq n$ were estimated in a way to satisfy the following equations

$$\alpha_{1i} + \alpha_{2i} + \beta_i + \alpha_{1i}^v + \alpha_{2i}^v + \beta_i^v = 1\,,\ 1 \leq i \leq n. \tag{A1}$$

$$\alpha_{2i} = 0.1\,\alpha_{1i}\,,\ \beta_i = 0.6\,\alpha_{1i}\,,\ \forall\, 1 \leq i \leq n \tag{A2}$$

$$\alpha_{ki}^v = 0.8\,\alpha_{ki}\,,\ k = 1, 2\,,\ \beta_i^v = 0.8\,\beta_i\,,\ \forall\, 1 \leq i \leq n \tag{A3}$$

with respect to the value of R_0. The infection probability among vaccinated susceptible δ was chosen such that $1 - \delta = 0.9$ represents the vaccine efficiency. Both incubation and hospitalization rates ψ and η were taken from the literature. Removal rates for both vaccinated and unvaccinated groups r_i and r_i^v for all $1 \leq i \leq n$ were estimated based on experimental data. Then, to determine the remaining parameters, the following assumptions were used

$$q_{1i} = (1 - \eta)\,\psi\,,\ q_{2i} = \eta\,\psi\,,\ \forall\, 1 \leq i \leq n$$

$$q_{1i}^v = (1 - 0.1\,\eta)\,\psi\,,\ q_{2i}^v = 0.1\,\eta\,\psi\,,\ \forall\, 1 \leq i \leq n$$

The initial conditions used are based on real data of Tunisia, Senegal, and USA populations at the beginning of vaccination campaigns at March 1^{st}, 2021, February 24, 2021, and December 12, 2020 respectively.

- The initial condition for Tunisia

- The initial condition for Senegal

- The initial condition for USA

$$\begin{aligned}
S(0) &= (0.169, 0.188, 0.181, 0.173, 0.147, 0.064)\\
E(0) &= (0.00555, 0.00615, 0.00593, 0.00567, 0.00482, 0.00209)\\
I_1(0) &= (0.00537, 0.00594, 0.00573, 0.00548, 0.00465, 0.00199)\\
I_2(0) &= (2.93276\ 10^{-7}, 1.62375\ 10^{-6}, 3.4463\ 10^{-6}, 8.69563\ 10^{-6}, 1.47812\ 10^{-5}, 2.89039\ 10^{-5})\\
R(0) &= (0.00347, 0.00384, 0.00370, 0.00354, 0.00301, 0.00130)\\
S^v(0) &= E^v(0) = I_1^v(0) = I_2^v(0) = R^v(0) = 0_{\mathbb{R}6}
\end{aligned}$$

The contact matrices D used are estimated and updated for 6 age groups for Tunisia, Senegal, and the USA by using data from [23].

TABLE A1 Epidemiological and demographic data

Parameter Description	Country		
	Tunisia	**Senegal**	**USA**
Population size[22]	11818619	16743928	331002647
Age class distribution P_i[22]	24,3%, 21,3%, 23,4%,17,7%, 10,2%, 3,1%	42,5%,27,3%, 16,7%,8,6%, 4%,0.7%	18%,20%, 20%,19%, 16%,7%
Infection rate α_{1i}	0,326797	0,326797	0,326797
Infection rate α_{2i}	$0, 1.\alpha_1$	$0, 1.\alpha_1$	$0, 1.\alpha_1$
Infection rate β_i	$(3/5).\alpha_1$	$(3/5).\alpha_1$	$(3/5).\alpha_1$
Infection rate β_i^v	$0, 8.\beta$	$0, 8.\beta$	$0, 8.\beta$
Infection rate α_{1i}^v	$0, 8.\alpha_1$	$0, 8.\alpha_1$	$0, 8.\alpha_1$
Infection rate α_{2i}^v	$0, 8.\alpha_2$	$0, 8.\alpha_2$	$0, 8.\alpha_2$
Infection probability among δ vaccinated susceptible	0.3	0.3	0.3
Incubation rate λ	0.2	0.2	0.2
Hospitalisation rate η[24]	0.0027, 0.0137, 0.03, 0.0792, 0.1585, 0.7158	0.0027, 0.0137, 0.0301, 0.0792, 0.1584, 0.7158	0.0027, 0.0137, 0.03005, 0.0792, 0.1585, 0.7158
Infection rate $q1$	0.19999, 0.19995, 0.19988 0.19968, 0.19937, 0.19714	0.19999, 0.19995, 0.19988 0.19968, 0.19937, 0.19714	0.19999, 0.19995, 0.19988 0.19968, 0.19937, 0.19714
Infection rate $q2$	$1.09\ 10^{-5}, 5.46\ 10^{-5}, 1.202\ 10^{-4}$ $3.169\ 10^{-4}, 6.339\ 10^{-4}, 2.8634\ 10^{-3}$	$1.09\ 10^{-5}, 5.46\ 10^{-5}, 1.202\ 10^{-4}$ $3.169\ 10^{-4}, 6.339\ 10^{-4}, 2.8634\ 10^{-3}$	$1.09\ 10^{-5}, 5.46\ 10^{-5}, 1.202\ 10^{-4}$ $3.169\ 10^{-4}, 6.339\ 10^{-4}, 2.8634\ 10^{-3}$
Infection rate q_1^v	0.199998, 0.199995, 0.199988 0.199968, 0.199937, 0.199714	0.199998, 0.199995, 0.199988 0.199968, 0.199937, 0.199714	v 0.199968, 0.199937, 0.199714
Infection rate q_2^v	$1.09\ 10^{-6}, 5.46\ 10^{-6}, 1.202\ 10^{-5}$ $3.169\ 10^{-5}, 6.339\ 10^{-5}, 2.8634\ 10^{-4}$	$1.09\ 10^{-6}, 5.46\ 10^{-6}, 1.202\ 10^{-5}$ $3.169\ 10^{-5}, 6.339\ 10^{-5}, 2.8634\ 10^{-4}$	$1.09\ 10^{-6}, 5.46\ 10^{-6}, 1.202\ 10^{-5}$ $3.169\ 10^{-5}, 6.339\ 10^{-5}, 2.8634\ 10^{-4}$
Recovered rate of I_{1i} r_{1i}	1/8	1/8	1/8
Recovered rate of I_2, r_2[13]	1/13.5, 1/13.5, 1/14, 1/14.5, 1/14.5, 1/15	1/13.5, 1/13.5, 1/14, 1/14.5, 1/14.5, 1/15	1/13.5, 1/13.5, 1/14, 1/14.5, 1/14.5, 1/15
Natural mortality rate	0, 0, 0.0001, 0.0005, 0.034, 0.072	0, 0, 0.0001, 0.0005, 0.034, 0.072	0, 0, 0.0001, 0.0005, 0.034, 0.072

ACKNOWLEDGMENTS

This work was supported in part by the French Ministry for Europe and Foreign Affairs via the project "REPAIR COVID-19-Africa" coordinated by the Pasteur International Network association and by European Union's Horizon 2020 research and innovation program under grant agreement No. 883441 (STAMINA).
We would also like to thank Pr. Joel S. Brown for his valuable assistance that contributed to enhancing the quality of this paper.

CONFLICT OF INTEREST

On behalf of all authors, the corresponding author states that there is no conflict of interest.

REFERENCES

1. Cheong KH, Jones MC. Introducing the 21st Century's New Four Horsemen of the Coronapocalypse. *Bioessays.* 2020;42.
2. Price A, Contreras-Suárez D, Zhu A, et al. The impact of ongoing COVID-19 lockdown on family finances and mental health. *medRxiv.* 2021.
3. global-covid-19-vaccination-mid-2022. 2022. https://reliefweb.int/report/world/strategy-achieve-global-covid-19-vaccination-mid-2022.
4. Dutta S. What is the impact of the SARS-CoV-2 omicron wave in South Africa?. *News-Medical.* 2022.
5. Babajanyan SG, Cheong KH. Age-structured SIR model and resource growth dynamics: a COVID-19 study. *Nonlinear Dyn.* 2021;104.
6. Linton NM, Kobayashi T, Yang Y, et al. Incubation period and other epidemiological characteristics of 2019 novel coronavirus infections with right truncation: a statistical analysis of publicly available case data. *Journal of clinical medicine.* 2020;2(9).
7. Anita S, Banerjeeb M, Ghoshb S, Volpertc V. Vaccination in a two-group epidemic model. *medRxiv.* 2021;2.
8. Colombo RM, Garavello M, Marcellini F, Rossi E. An age and space structured SIR model describing the Covid-19 pandemic. *Journal of mathematics in industry.* 2020;1(10):1-20.
9. Fall A, Iggidr A, Sallet v, Tewa J. Epidemiological Models and Lyapunov Functions. *Journal of mathematics in industry.* 2007;1(2):62-83.
10. Radulescu A, Williams C, Cavanagh K. Management strategies in a SEIR-type model of COVID 19 community spread,. *Nature.* 2020;1(10):1-16.
11. Driessche v. dP, Watmough J. Reproduction numbers and sub-threshold endemic equilibria for compartmental models of disease transmission. *Mathematical Biosciences.* 2002;1-2(180):29-48.
12. Laarabi H, Abta A, Hattaf K. Optimal Control of a Delayed SIRS Epidemic Model with Vaccination and Treatment. *Acta Biotheor.* 2015;2(63):87-97.
13. Voinsky I, Baristaite G, Gurwitz D. Effects of age and sex on recovery from COVID-19: Analysis of 5769 Israeli patients. *Journal of Infection.* 2020;2(81):e102-e103.
14. Bentout S, Tridane A, Djilali S, Touaoula TM. Age-Structured Modeling of COVID-19 Epidemic in the USA, UAE and Algeria. *Alexandria Engineering Journal.* 2020.
15. Ram V, Schaposnik LP. A modified age-structured SIR model for COVID-19 type viruses. *Scientific reports.* 2021.
16. Jaouimaa F, Dempsey D, Van Osch S, et al. An age-structured SEIR model for COVID-19 incidence in Dublin, Ireland with framework for evaluating health intervention cost. *Plos one.* 2021.
17. Verrelli CM, Della Rossa F. Two-Age-Structured COVID-19 Epidemic Model: Estimation of Virulence Parameters to Interpret Effects of National and Regional Feedback Interventions and Vaccination,. *mathematics.* 2021.
18. Weyand C, Goronzy J. Aging of the Immune system: Mechanisms and Therapeutic Targets. *Ann Am Thorac Soc.* 2016;5:S422-S428.
19. Chhetri B, Vamsi D, Sanjeevi C. Optimal Control Studies on Age Structured Modeling of COVID-19 in Presence of Saturated Medical Treatment of Holling Type III. *Differ Equ Dyn Syst.* 2022.
20. Beal L, Hill D, Martin R, Hedengren JD. GEKKO Optimization Suite. *Processes.* 2018;8(6):e102-e103.
21. Lenhart S, Workman J. *Optimal Control Applied to Biological Models,*. New York: Chapman and Hall, 2007.
22. Population Pyramids of the World from 1950 to 2100, Population Pyramid.net. 2020. https://www.populationpyramid.net/tunisia/2020/.
23. Prem K, Cook AR, Jit M. Projecting social contact matrices in 152 countries using contact surveys and demographic data. *PLoS computational biology.* 2017;9(13):e1005697.
24. Stratégie vaccinale contre la COVID-19 en Tunisie. http://www.santetunisie.rns.tn/images/strategie-vaccination-covid-19.pdf.